

ПАРАМЕТРЫ ПЛАЗМЫ И КИНЕТИКА ТРАВЛЕНИЯ КРЕМНИЯ В СМЕСИ $CF_4 + C_4F_8 + O_2$: ЭФФЕКТ СООТНОШЕНИЯ CF_4/C_4F_8

А.М. Ефремов, А.В. Бобылев, К.-Н. Кwon

Александр Михайлович Ефремов (ORCID 0000-0002-9125-0763)*, Александр Викторович Бобылев (ORCID 0009-0009-3526-6822)

Ивановский государственный химико-технологический университет, Шереметевский пр., 7, Иваново, Российская Федерация, 153000

E-mail: amefremov@mail.ru*, prototyp16@mail.ru

Kwang-Ho Kwon (ORCID 0000-0003-2580-8842)

Korea University, 208 Seochang-Dong, Chochiwon, Korea, 339-800

E-mail: kwonkh@korea.ac.kr

Исследовано влияние соотношения фторуглеродных компонентов в плазмообразующей смеси $CF_4 + C_4F_8 + O_2$ на электрофизические параметры плазмы, стационарные концентрации активных частиц и кинетику травления кремния в условиях, типичных для реактивно-ионных процессов. Совместное использование методов диагностики (двойной зонд Ленгмюра, оптическая эмиссионная спектроскопия) и моделирования плазмы подтвердило известные особенности химии плазмы в индивидуальных фторуглеродных газах в присутствии кислорода, а также позволило провести детальный анализ кинетики атомов фтора и кислорода для трехкомпонентной смеси. Было показано, что замещение CF_4 на C_4F_8 при постоянном содержании O_2 а) вызывает слабые возмущения параметров электронной и ионной компонент плазмы (температуры электронов, концентрации электронов и плотности потока энергии ионов); б) обеспечивает резкое увеличение концентрации полимеробразующих радикалов CF_x ($x = 1, 2$); в) приводит к монотонному снижению концентрации атомов F. Последний эффект обусловлен одновременным изменением как скорости образования атомов, так и частоты их гибели, что особенно проявляется в смесях с высоким содержанием C_4F_8 . В экспериментах установлено, что скорость травления Si более чем на 85% определяется ее химической составляющей (в форме ионно-стимулированной гетерогенной реакции $Si + xF \rightarrow SiF_x$) и снижается с увеличением доли C_4F_8 в исходном газе. Наблюдаемое при этом изменение эффективной вероятности реакции не согласуется с ростом скорости осаждения полимера и толщины полимерной пленки (как это следует из изменения параметров газовой фазы), но может быть связано с ослаблением пассивации поверхности атомами кислорода.

Ключевые слова: CF_4 , C_4F_8 , O_2 , плазма, параметры, активные частицы, ионизация, диссоциация, травление, полимеризация

PLASMA PARAMETERS AND SILICON ETCHING KINETICS IN $CF_4 + C_4F_8 + O_2$ MIXTURE: EFFECT OF CF_4/C_4F_8 MIXING RATIO

A.M. Efremov, A.V. Bobylev, K.-H. Kwon

Alexander M. Efremov (ORCID 0000-0002-9125-0763), Alexander V. Bobylev (ORCID 0009-0009-3526-6822)

Ivanovo State University of Chemistry and Technology, Sheremetevskiy ave., 7, Ivanovo, 153000, Russia

E-mail: amefremov@mail.ru*, prototyp16@mail.ru

Kwang-Ho Kwon (ORCID 0000-0003-2580-8842)

Korea University, 208 Seochang-Dong, Chochiwon, Korea, 339-800

E-mail: kwonkh@korea.ac.kr

In this work, we investigated the influence of fluorocarbon component ratio in the $CF_4 + C_4F_8 + O_2$ gas mixture on electro-physical plasma parameters, steady-state densities of active species and silicon etching kinetics under typical reactive-ion process conditions. The combination of plasma diagnostics (double Langmuir probes, optical emission spectroscopy) and plasma modeling confirmed known peculiarities of plasma chemistry of individual fluorocarbons in the presence of oxygen as well as provided an extended analysis of both fluorine and oxygen atom kinetics in the three-component gas mixture. It was shown that the substitution of CF_4 by C_4F_8 at the constant fraction of O_2 a) causes the weak disturbance in electrons- and ions-related plasma parameters (electron temperature, electron density, ion energy flux); b) provides drastically increasing density of polymerizing CF_x ($x = 1, 2$) radicals; and c) results in monotonically decreasing F atoms density. The latter is due to simultaneous changes in both F atom formation rate and their loss frequency, especially in C_4F_8 -rich plasmas. From experiments, it was found that Si etching rate is by more than 85% controlled by its chemical component (in a form of ion-stimulated heterogeneous reaction $Si + xF \rightarrow SiF_x$) and decreases with increasing C_4F_8 fraction in a feed gas. The change in effective reaction probability contradicts with the growth of polymer deposition rate and film thickness (as it follows from changes in gas-phase plasma characteristics) but may reflect the weakening of surface passivation by oxygen atoms.

Keywords: CF_4 , C_4F_8 , O_2 , plasma, parameters, active species, ionization, dissociation, etching, polymerization

Для цитирования:

Ефремов А.М., Бобылев А.В., Kwon К.-Н. Параметры плазмы и кинетика травления кремния в смеси $CF_4 + C_4F_8 + O_2$: эффект соотношения CF_4/C_4F_8 . *Изв. вузов. Химия и хим. технология*. 2024. Т. 67. Вып. 6. С. 29–37. DOI: 10.6060/ivkkt.20246706.6982.

For citation:

Efremov A.M., Bobylev A.V., Kwon K.-H. Plasma parameters and silicon etching kinetics in $CF_4 + C_4F_8 + O_2$ mixture: effect of CF_4/C_4F_8 mixing ratio. *ChemChemTech [Izv. Vyssh. Uchebn. Zaved. Khim. Khim. Tekhnol.]*. 2024. V. 67. N 6. P. 29–37. DOI: 10.6060/ivkkt.20246706.6982.

INTRODUCTION

During the last decade, gaseous fluorocarbons played an important role in micro- and nano-electronics technology being used for the reactive-ion etching (RIE) of silicon and silicon-based compounds [1, 2]. In fact, namely the RIE process, as a part of the standard photolithography cycle, provides the patterning of various functional layers, determines feature sizes for integrated components and finally, influences the overall device performance [2, 3]. Modern RIE technology frequently uses inductively-coupled plasma (ICP) etching systems operating with two power sources: one is to excite the plasma and to control densities of active species while another one is to produce the negative bias on the etched surface and thus, to set the ion bombardment energy. Accordingly, the independent adjustment of physical and chemical etching pathways allows one to enlarge the “window” for output RIE characteristics and thus, to improve both the overall device structure and performance [3, 4].

In many previous works, it was clearly shown that output RIE characteristics, such as etching rate, etching anisotropy and selectivity in respect to over-

and under-layer materials, strongly depend on the polymerizing ability of fluorocarbon gas, and the latter is characterized by the y/x ratio in the original C_xF_y molecule [5-8]. In particular, the CF_4 ($z/x = 4$) plasma is featured by minimum polymerizing ability, as it combines the high density of F atoms and the low density of CF_x ($x = 1, 2$) radicals [9-11]. Under typical RIE conditions, such situation produces high etching rates and good surface clearness, but results in the isotropic (with a sufficient overcut) patterning of silicon and its low etching selectivity in respect to SiO_2 [4, 5]. Oppositely, the C_4F_8 ($z/x = 2$) plasma exhibits maximum polymerizing ability due to the domination of CF_x over F species in a gas phase [9, 10, 12]. As such, one normally obtains lower etching rates with higher surface residues (due to the deposition of thick continuous fluorocarbon polymer film), anisotropic etching profiles (due to the passivation of side walls by the polymer film) [6, 8] and the decent SiO_2/Si etching selectivity (due to the thicker polymer film on the oxygen-free surface that causes the worse access for F atoms) [7, 8].

The widely known method to satisfy the given process requirements in respect to etching/polymerization balance is the use of additive gas which enforces or suppresses the polymerization [5]. For instance, the

addition of hydrogen causes an increase in both polymer deposition rate and film thickness due to the formation of more polymerizing CH_x radicals and decreasing F atom density through their conversion into HF species [5, 13, 14]. Oppositely, the addition of oxygen transforms CF_x radicals in forms of non-polymerizing CF_xO and CO_x compounds, increases the F atom density as well as initiates the oxidative destruction of deposited polymer film [5, 15, 16]. In our previous works [17-19], we have performed the comparative study of $\text{CF}_4 + \text{O}_2$ and $\text{C}_4\text{F}_8 + \text{O}_2$ plasmas under identical operating conditions. It was found that and increase in O_2 fraction in a feed gas always a) causes the rather weak disturbance in electrons- and ions-related plasma parameters; b) suppresses densities of CF_x radicals through the $\text{CF}_x + \text{O}/\text{O}(\text{D}) \rightarrow \text{CF}_{x-1}\text{O} + \text{F}$ reaction family; and c) results in non-monotonic (with maxima at $\sim 30\%$ O_2 in CF_4 -based plasma and $\sim 80\%$ O_2 in C_4F_8 -based plasma [19]) changes in F atom density. At the same time, the last effect has the different nature and is connected with either similar behavior of total F atom formation rate or decreasing their loss frequency. Another important finding was that an excess of oxygen (for example, more than 50% in $\text{C}_4\text{F}_8 + \text{O}_2$ mixture) lowers the reaction probability for F atoms through the oxidation of silicon and/or reaction products into lower volatile SiF_xO_y compounds [18, 19]. Therefore, the alternate way to control both etching and polymerization kinetics at lower O_2 contents is required.

The main idea of given work was to take the three-component $\text{CF}_4 + \text{C}_4\text{F}_8 + \text{O}_2$ gas mixture with a fixed 50% O_2 and then, to study the effect of fluorocarbon gas mixing ratio on gas-phase plasma characteristics, etching/polymerization balance and Si etching process. Accordingly, main goals were a) to investigate how $\text{CF}_4/\text{C}_4\text{F}_8$ mixing ratio does influence electrons- and ions related plasma parameters; b) to determine corresponding changes in kinetics and densities of both fluorine atoms and polymerizing radicals; and c) to analyze the Si etching kinetics in terms of effective reaction probability.

EXPERIMENTAL AND MODELING DETAILS

Experimental setup and procedures

Both plasma diagnostics and etching experiments were carried out in the planar (with the upper-side flat coil) inductively coupled plasma (ICP) reactor known from our previous works [17-19]. Plasma was excited using the 13.56 MHz rf generator connected to the coil through the matching network while another 13.56 MHz rf source powered the chuck electrode used as the substrate holder. The latter allowed one to control the ion bombardment energy (ϵ_i) through the

change in the negative dc bias voltage ($-\text{U}_{\text{dc}}$). Constant processing conditions were total gas flow rate ($q = 40$ sccm), gas pressure ($p = 6$ mTorr), input power ($W_{\text{inp}} = 700$ W) and bias power ($W_{\text{dc}} = 200$ W). The variable parameter was the $\text{CF}_4/\text{C}_4\text{F}_8$ mixing ratio that was set by adjusting partial flow rates for corresponding gases at fixed O_2 flow rate of 20 sccm. Accordingly, the fraction of oxygen in a feed gas ($y(\text{O}_2) = q(\text{O}_2)/q$) was always 50% while and increase in $q(\text{C}_4\text{F}_8)$ from 0-20 sccm ($y(\text{C}_4\text{F}_8) = 0$ -50%) corresponded to the full substitution of CF_4 by C_4F_8 .

Plasma diagnostics was represented by double Langmuir probe (LP) measurements (DLP2000, Plasmart Inc.) and optical emission spectroscopy (OES) (AvaSpec-3648, JinYoung Tech).

In LP measurements, the probe head was introduced through the viewport on the chamber wall and was centered in the radial position. To minimize the distortion of voltage-current curves due to the deposition of fluorocarbon polymer on probe tips, these were exposed to 50% Ar + 50% O_2 plasma for ~ 5 min before and after each measurement. Previously, we have demonstrated the efficiency of such cleaning method to provide correct plasma diagnostics data in high polymerizing fluorocarbon gases [18, 19]. The treatment of voltage-current curves was based on well-known statements of Langmuir probe theory for low pressure discharges [5, 20]. The results were electron temperature (T_e) and ion current density (J_+).

In OES measurements, the plasma emission was analyzed through the same sidewall viewport with pre-installed quartz window. To obtain the information on steady-state densities of F atoms, we fulfilled the $\text{CF}_4 + \text{C}_4\text{F}_8 + \text{O}_2$ gas mixture by 2 sccm ($\sim 4.5\%$) of Ar and then, monitored emission intensities (I) for two widely known actinometrical lines, such as Ar 750.4 nm ($\epsilon_{\text{th}} = 13.48$ eV) and F 703.8 nm ($\epsilon_{\text{th}} = 14.75$ eV). Both lines exhibit low radiational lifetimes as well as featured by direct electron impact excitation mechanisms with known process cross-sections [21]. Accordingly, the standard actinometrical approach [21, 22] yields the F atom density as $[\text{F}] = [\text{Ar}]C_a(I_{\text{F}}/I_{\text{Ar}})$, where $[\text{Ar}] = y_{\text{Ar}}N$ is the Ar density, y_{Ar} is the Ar fraction in a feed gas, C_a is the actinometrical coefficient (~ 2.0 at $T_e = 3$ -6 eV [21]), and $N = p/k_{\text{B}}T_{\text{gas}}$ is the total gas density at the given gas temperature T_{gas} . Similarly to our previous works [17-19], the latter was assumed to be independent on gas mixing ratio and equal to ~ 600 K. This value is quite typical for ICP reactors of given geometry operated with input power densities of ~ 0.5 W/cm³ [23]. In preliminary experiments, it was found that the presence of Ar (at least, in the amount used in this work) does not disturb plasma parameters,

and thus does not influence the F atom kinetics. As such, F atom densities obtained after the actinometry procedure may surely be associated with those in Ar-free plasmas.

In etching experiments, we used fragments of standard Si (111) wafer with an average size of $\sim 2 \times 2$ cm. The small sample surface area allowed one to exclude the loading effect (in other words, to realize the etching regime controlled by heterogeneous process kinetics) as well as to minimize the influence of reaction products on gas-phase plasma characteristics. Accordingly, there were no principal (i.e. exceeding the typical experimental error) differences in plasma diagnostics data obtained with and without sample loading. Etched samples were placed in the middle part of chuck electrode, and the chuck temperature (T_s) was stabilized at ~ 20 °C using the built-in water-flow cooling system. After processing, the thickness of removed Si layer (the so-called etching depth, Δh) was determined using the surface profiler (Alpha-Step 500, Tencor). For this purpose, we developed a partial surface masking by the photoresist AZ1512 with a thickness of ~ 1.5 μm . As nearly linear $\Delta h = f(\tau)$ curves suggested the steady-state etching regime, Si etching rate was simply calculated as $R = \Delta h/\tau$, where $\tau = 1$ min is the processing time.

Approaches for the analysis of plasma chemistry

To obtain the information on densities of plasma active species, we used a simplified 0-dimensional (global) model operating with volume-averaged plasma parameters. Both modeling algorithm and kinetic scheme (the set of reaction with corresponding rate coefficients) were taken from our previous works dealt with $\text{CF}_4 + \text{O}_2$ and $\text{C}_4\text{F}_8 + \text{O}_2$ [17-19] plasmas. Basic assumptions were as follows:

1) The electron energy distribution function (EEDF) may surely be associated with Maxwellian one. The latter is due to the sufficient contribution of equilibrium energy exchanges in electron-electron collisions under conditions of high-density ($n_+ > 10^{10} \text{ cm}^{-3}$) plasmas [5]. Accordingly, rate coefficients for electron-impact reactions are available from fitting expressions $k = f(T_e)$ [11, 12, 16, 17, 24, 25].

2) The low electronegativity of all three component gases at $p < 20$ mTorr provides $n_+ \approx n_e$, where n_e is the electron density [16, 24, 25]. Physically, such situation is provided by both high ionization degree for gas species and low efficiency of dissociative attachment at low pressures. As a result, the relationship between measured J_+ and total density of positive ions n_+ may simply be assumed as $J_+ \approx 0.61en_+(eT_e/m_i)^{1/2}$ [5], where m_i is the effective ion mass. The last parameter was evaluated through individual masses of dominant positive ions, as described in Refs. [18, 19].

3) The heterogeneous recombination of atoms and radicals follows the first-order kinetics, and corresponding reaction probabilities [24, 25] are independent on the fluorocarbon component mixing ratio. The indirect proofs are a) the nearly constant temperature of external chamber wall that allows one to expect the negligible change in the internal wall temperature; and b) no principal changes in the internal wall condition, as only the re-deposition of fluorocarbon polymer film takes place.

The input model parameters were experimental data on T_e and J_+ measured at different $\text{CF}_4/\text{C}_4\text{F}_8$ mixing ratios. As outputs, the model yielded steady-state densities of plasma active species and their fluxes at the plasma/surface interface.

Approaches for the analysis of etching and polymerization kinetics

The features of heterogeneous processes kinetics in polymerizing plasmas have been studied and discussed in several works, such as Refs. [6-8, 26]. Based on this data, we suggested a set of gas-phase-related parameters to trace relative changes in etching rate, polymer deposition rate and polymer film thickness [15, 18, 19]. The general idea may briefly be summarized in a form of following statements:

1) Any physical etching pathway (sputtering of target surface, destruction of chemical bonds between surface atoms or desorption of low volatile reaction products) has the rate of $Y_S \Gamma_+$, where Y_S is the process yield (particle per incident ion), and $\Gamma_+ \approx J_+/e$ is the ion flux. Corresponding process rate may be traced by the parameter $G1 = (M_i \epsilon_i)^{1/2} \Gamma_+$, where the first multiplier characterizes the momentum transferred from the incident ion to the surface atom.

2) Any chemical etching pathway (the interaction of silicon with F atoms or the etching of fluorocarbon polymer film by O atoms) has the rate of $\gamma_R \Gamma_X$, where γ_R is the effective reaction probability, and $\Gamma_X \approx 0.25[X](RT_{\text{gas}}/\pi M_X)^{1/2}$ is the flux of corresponding atomic species. The spontaneous reaction mechanism assumes $\gamma_R = \text{const}$ at constant surface temperature.

3) The growth of fluorocarbon polymer film is provided by CF_x ($x < 3$) radicals and appears to be faster in fluorine-poor plasmas. Therefore, the change in the polymer deposition rate may be traced by the parameter $G2 = \Gamma_{\text{pol}}/\Gamma_F$, where Γ_{pol} is the total flux of CF_2 and CF radicals while Γ_F is the flux of F atoms.

4) The destruction of fluorocarbon polymer film is provided by both physical and chemical pathways. Corresponding changes in the polymer film thickness may be traced by $G3 = G2/G1$ and $G4 = G2/\Gamma_O$, where Γ_O is the flux of oxygen atoms.

5) The Si etching rate under RIE conditions represents the total effect from physical sputtering (R_{phys}) and heterogeneous chemical reaction with F atoms (R_{chem}). Accordingly, the parameter $G5 = \Gamma_{\text{F}}/G1$ traces the balance between directional and chaotic etching mechanisms as well as characterizes the change of etching anisotropy.

RESULTS AND DISCUSSION

From plasma diagnostics by Langmuir probes, it was found that effects of $\text{CF}_4/\text{C}_4\text{F}_8$ mixing ratio on electrons- and ions-related plasma parameters (Table 1) adequately reflects differences between $\text{CF}_4 + \text{O}_2$ and $\text{C}_4\text{F}_8 + \text{O}_2$ plasmas mentioned in our previous work [19]. With accounting for plasma composition data shown in Fig. 1, most important findings may briefly be summarized as follows:

Table 1

Electrons- and ions-related plasma parameters

Таблица 1. Параметры электронной и ионной компонент плазмы

$y(\text{C}_4\text{F}_8)$, %	T_e , eV	J_+ , mA/cm ²	$n_+ \approx n_e$, 10^{10} cm ⁻³	$-U_{dc}$, V	$G1$, 10^{17}
0	3.8	0.93	3.02	280	6.13
25	4.2	0.95	2.92	281	6.23
50	4.4	0.98	2.89	282	6.39

Note: $G1 = (M_{\text{ie}})^{1/2} \Gamma_+ (eV^{1/2} \text{cm}^{-2} \text{s}^{-1})$

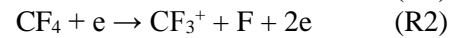
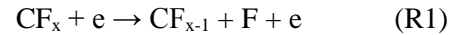
Примечание: $G1 = (M_{\text{ie}})^{1/2} \Gamma_+ (3B^{1/2} \text{cm}^{-2} \text{c}^{-1})$

1) A monotonic increase in the electron temperature surely means a decrease in overall electron energy losses toward C_4F_8 -rich plasmas. Though the dominant energy loss channel at 0-50% C_4F_8 seems to be collisions of electrons with CF_2O molecules, one can also obtain “the substitution” of F_2 , O_2 and CO_2 by CF_x ($x = 2, 3, 4$) components in a gas phase. As follows from Refs. [27, 28], the first group of species is characterized by lower-threshold excitations processes (and thus, provides the wider electron energy loss range) as well as exhibit higher cross-sections for both vibrational and electronic excitations. Accordingly, an increase in $y(\text{C}_4\text{F}_8)$ enriches EEDF by high-energy electrons and causes the growth of their mean energy.

2) A weak decrease in both positive ion and electron densities reflects, probably, an increase in their loss frequencies (due to increasing both electron diffusion coefficient and ion Bohm velocity together with T_e) under the condition of nearly constant total ionization rate. The latter is mostly contributed by CF_2O (as the corresponding $k_{iz}[\text{CF}_2\text{O}]$ value exceeds those for other species, where k_{iz} is the ionization rate coefficient) while increasing tendencies for $k_{iz} = f(T_e)$ are compensated by the appearance of harder ionizing CF_x components.

3) The nearly constant ion flux $\Gamma_+ \approx J_+/e$ and ion bombardment energy (as follows from the behavior of $-U_{dc}$) provide the very weak change in the parameter $G1$ characterizing the ion bombardment intensity. As such, no principal effects of $\text{CF}_4/\text{C}_4\text{F}_8$ mixing ratio on ion-driven heterogeneous processes are expected.

Basic features of non-oxygenated CF_4 plasma in respect to densities of neutral particles have been studied in detail in previous works [9-11, 15]. When taking in mind the results obtained exactly at given experimental conditions [9, 15], one can surely assume $[\text{CF}_x] > [\text{CF}_{x-1}]$ (due to the stepwise decomposition of fluorocarbon species in the R1 reaction family) and $[\text{F}] \approx [\text{CF}_3]$. The latter is because dominant formation pathways for fluorine atoms, such as R1 for $x = 4$ and R2, also produce CF_3 radicals. In addition, about ~10% of total F atom production rate is contributed by R3. The reasons are the essential density of source species (due to their effective formation in R4 on chamber walls) as well as the low dissociation threshold (~4.3 eV) that provides high rate coefficient ($k_3 \sim 2.4 \times 10^{-9}$ cm³/s vs. $k_1 \sim 2.5 \times 10^{-10}$ cm³/s and $k_2 \sim 5.7 \times 10^{-10}$ cm³/s). Accordingly, heterogeneous processes R4 and R5 are main loss pathways for fluorine atoms and fluorocarbon radicals.



The addition of O_2 initiates the conversion of CF_x radicals into CF_2O , CFO , CO and CO_2 species in R6 ($k_6 \sim 6.1 \times 10^{-11}$ cm³/s for $x = 1$ and $\sim 3.2 \times 10^{-11}$ cm³/s for $x = 2, 3$), causes the drastic decrease in $[\text{CF}_x]$ (by more than 100 times at $y(\text{O}_2) = 50\%$) as well as provides the domination of CF_2O over other gas-phase components in 50% $\text{CF}_4 + 50\%$ O_2 plasma (Fig. 1). The latter is supported by the effective formation of CF_2O molecules in R6, R7 ($k_7 \sim 1.0 \times 10^{-11}$ cm³/s), R8 ($k_8 \sim 8.0 \times 10^{-11}$ cm³/s) and R9 ($k_9 \sim 1.1 \times 10^{-11}$ cm³/s for $x = 2$ and $\sim 7.0 \times 10^{-13}$ cm³/s for $x = 1$). Another remarkable oxygen-related effect is the increasing density of F_2 molecules (by more than an order of magnitude at 50% O_2 compared with pure CF_4 plasma) through both R3 and R10 ($k_{10} \sim 2.0 \times 10^{-11}$ cm³/s). As a result, the leading role in the formation of F atoms is transferred from the dissociation of CF_x radicals to R3, R11, R12, R13 ($k_{13} \sim 2.5 \times 10^{-11}$ cm³/s), R14 ($k_{14} \sim 5.0 \times 10^{-11}$ cm³/s) and R15 ($k_{15} \sim 1.0 \times 10^{-10}$ cm³/s). The corresponding increase in the total F atom formation rate sufficiently lifts up the $[\text{F}]$ value compared with pure CF_4 plasma. Definitely, this fact is known for a long time and has repeatedly

been confirmed by both plasma diagnostics and modeling [5, 16, 29, 30].

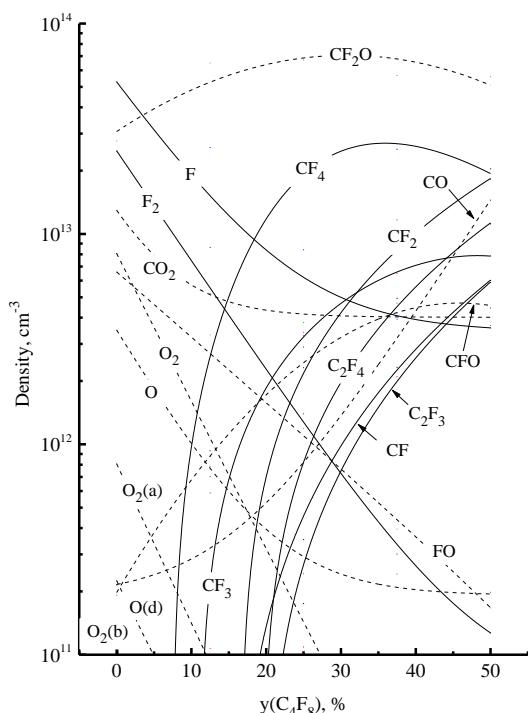
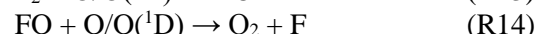
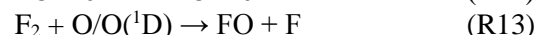
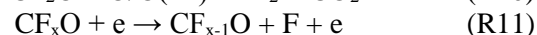
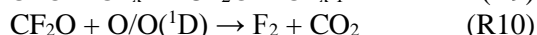
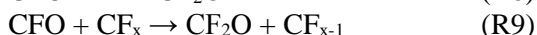
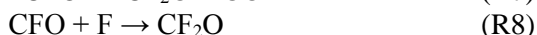
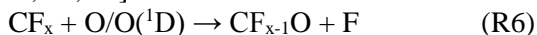
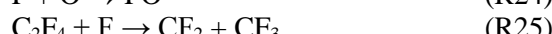
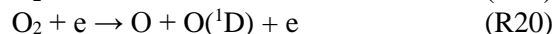
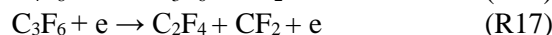
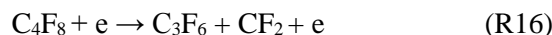


Fig. 1. Model-predicted densities of neutral species as functions of C_4F_8 fraction in a feed gas. Dashed lines are to highlight oxygen-containing components

Рис. 1. Расчетные концентрации нейтральных частиц в зависимости от доли C_4F_8 в плазмообразующем газе. Пунктирные линии выделяют кислородсодержащие компоненты

The substitution of CF_4 by C_4F_8 accelerates the formation of CF_x species (directly for CF_2 through R16, R17 and R18 while indirectly for other ones through both R1 and R5) as well as lowers their loss rates in R6. The latter is due to the lack of oxygen atoms that results from decreasing rates of R19 and R20. The reason is decreasing density of O_2 molecules (by more than three orders of magnitude, see Fig. 1) provided by the growth of their loss rate in R21 ($k_{21} \sim 3.2 \times 10^{-11} \text{ cm}^3/\text{s}$) and R22 ($k_{22} \sim 1.5 \times 10^{-11} \text{ cm}^3/\text{s}$). As a result, the plasma is enriched by non-oxygenated fluorocarbon components (mainly by CF_4 , CF_3 and CF_2 , as shown in Fig. 1). Two other remarkable phenomena

are rapidly decreasing $[\text{F}_2]$ and $[\text{FO}]$ values. The first is due to the acceleration of R23 ($k_{23} \sim 8.0 \times 10^{-14} \text{ cm}^3/\text{s}$ for $x = 2$ and $\sim 4.0 \times 10^{-12} \text{ cm}^3/\text{s}$ for $x = 1$) while the second one reflects a decrease in FO formation rate in heteronomous process R24. All these suppress the production of F atoms in R3 and R12–R14 as well as slightly lowers the total F atom formation rate that reaches the minimum at $y(\text{C}_4\text{F}_8) \sim 25\%$. The further increase in $y(\text{C}_4\text{F}_8)$ intensifies the generation of F atoms through R1 and R2, results in the growth of total F atom formation rate, but does not change the decreasing tendency for the F atom density. The reason is the increasing F atom decay rate in R25 ($k_{25} \sim 4.0 \times 10^{-11} \text{ cm}^3/\text{s}$) which appears to be faster compared with R4 and R5. Exactly the same mechanism controls the F atom density in the $\text{CF}_4 + \text{C}_4\text{F}_8$ plasma in the absence of oxygen [9, 10]. From Fig. 2, it can be seen also that model-predicted F atom densities are in good agreement with those obtained after the actinometry procedure. As the $[\text{F}]$ value is closely matched with densities of other species through the multi-channel reaction scheme, one can assume the correct understanding of main kinetic effects influencing the steady-state plasma composition.



From Fig. 3(a), it can be seen that measured Si etching rate, R , exhibits the monotonic decrease with increasing C_4F_8 fraction in a feed gas. Formally, such behavior contradicts with the change in the ion bombardment intensity as well as correlates with the F atom flux. In order to divide contributions of physical and chemical etching pathways, we evaluated $R_{\text{phys}} = Y_s \Gamma$ using experimental data on Si sputtering yields ($Y_s \approx 0.2 \text{ atom/ion}$ at ion energies of $\sim 300 \text{ eV}$ [31, 32]) and then, found the chemical etching component as $R_{\text{chem}} = R - R_{\text{phys}}$. The result was that $R_{\text{phys}} \approx \text{const}$ (14–15 nm/min at 0–50% C_4F_8) and $R_{\text{chem}} \gg R_{\text{phys}}$. Therefore, the prevailing etching mechanism under the given set of processing conditions is the heterogeneous chemical reaction R25.

Another principal finding is that a decrease in R_{chem} (by ~ 1.5 times for 0–50% C_4F_8) appears to much weaker compared with F atom flux (by ~ 15 times for

0-50% C₄F₈) that points out on increasing effective reaction probability $\gamma_R = R_{chem}/\Gamma_F$ (Fig. 3). In previous

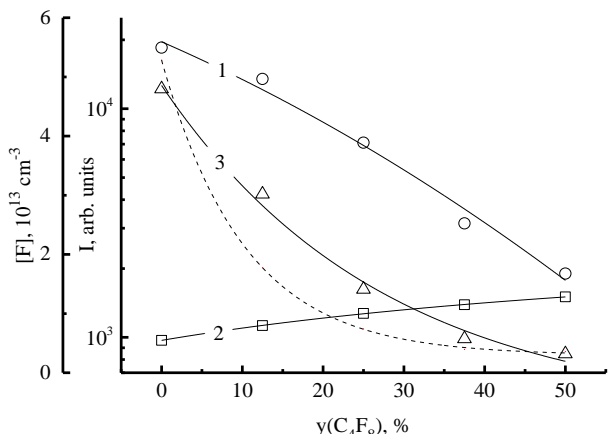
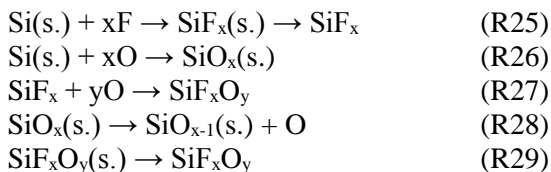


Fig. 2. Emission intensities for analytic lines (1 – F 703.8 nm, 2 – Ar 750.4 nm) and F atom density obtained after the actinometry procedure (3) as functions of C₄F₈ fraction in a feed gas. Dashed line repeats the model-predicted F atom density from Fig. 1
 Рис. 2. Интенсивности излучения аналитических линий (1 – F 703,8 нм, 2 – F 703,8 нм) и концентрации атомов фтора, полученные методом актинометрии (3), в зависимости от доли C₄F₈ в плазмообразующем газе. Пунктирная линия дублирует расчетную концентрацию атомов фтора с рис. 1

works [15, 18, 19], it was found that the parameter γ_R for silicon at the nearly constant surface temperature depends on two main factors, which are a) the thickness of the fluorocarbon polymer film influencing the access of F atoms to the etched surface (so that the rule of “the thicker film, the lower γ_R ” does work); and b) the competitive adsorption of O atoms that finally leads to the oxidation of silicon (R26) and/or the conversion of etching products into lower volatile SiF_xO_y compounds (R27). Obviously, the last two mechanisms reduce γ_R through the appearance of ion-assisted stages (R28, R29) and decreasing fraction of free adsorption sites for F atoms, as some of those appear to be occupied by both oxygen itself and oxygen-containing by-products.



From Tab. 2, it can be understood the substitution of CF₄ by C₄F₈ increases the total flux of polymerizing radicals Γ_{pol} , causes the sufficient growth of the polymer deposition rate (as follows from the change of G2) as well as promotes increasing amount of residual polymer on the etched surface (as follows from changes of G3 and G4). Therefore, one can reasonably expect the thicker polymer film and thus, the lower (but

not the higher, as follows from Fig. 3(a) γ_R in the C₄F₈-rich plasma. In our opinion, such situation takes place because the actual amount of oxygen is enough for the effective destruction of depositing polymer film, even if the surface is treated in 50% C₄F₈ + 50% O₂ plasma with the maximum polymerizing ability. As a result, the steady-state surface condition always corresponds to the very thin or non-continuous film which does not influence the kinetics of R25.

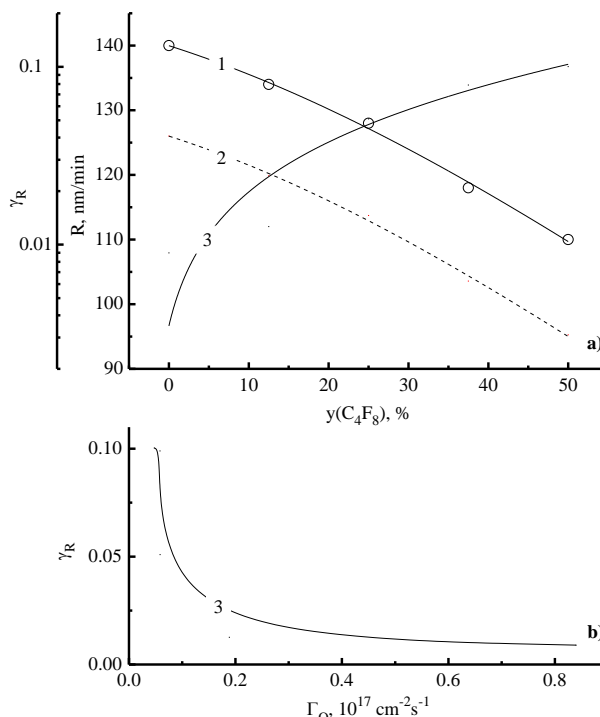


Fig. 3. Silicon etching rate (1) and effective reaction probability (3) as functions of C₄F₈ fraction in a feed gas. Dashed line (2) represents the rate of chemical etching component, R_{chem}
 Рис. 3. Скорость травления кремния (1) и эффективная вероятность взаимодействия (3) в зависимости от доли C₄F₈ в плазмообразующем газе. Пунктирная линия (2) представляет химическую составляющую скорости травления, R_{chem}

Table 2
Parameters characterizing heterogeneous process kinetics

Таблица 2. Параметры, характеризующие кинетику гетерогенных процессов

y(C ₄ F ₈), %	$\Gamma_{pol}, 10^{16} \text{ cm}^{-2}\text{s}^{-1}$	G2, 10 ⁻²	G3, 10 ⁻²⁰	G4, 10 ⁻¹⁸	G5
0	0.02	0.01	0.02	0.002	1.91
25	2.5	13.5	21.7	23.2	0.30
50	35.2	446.2	698.3	935.5	0.12

Note: G2 = Γ_{pol}/Γ_F ; G3 = G2/G1 (eV^{-1/2}cm²s); G4 = G2/Γ₀ (cm²s); and G5 = $\Gamma_F/G1$ (eV^{-1/2})

Примечание: G2 = Γ_{pol}/Γ_F ; G3 = G2/G1 (эВ^{-1/2}см²с); G4 = G2/Γ₀ (см²с); and G5 = $\Gamma_F/G1$ (эВ^{-1/2})

At the same time, one can mention the evident correlation between an increase in γ_R and decreasing

oxygen atom flux, as follows from the change in O atom density in a gas phase. When analyzing this phenomenon, one can reasonably expect that a decrease in Γ_O suppresses both R26 and R27, lowers the passivation of etched surface by oxygen-containing by-products as well as causes the growth of γ_R through increasing fraction of free adsorption sites for F atoms. Earlier, the same mechanism has been reported for $CF_4 + O_2$ plasma in the range of 0-75% O_2 as well as for $C_4F_8 + O_2$ plasma at $y(O_2) > 50\%$ [19]. Therefore, the results of given work are in agreement with previously published data. Finally, we would like to mention that the shape of $\gamma_R = f(\Gamma_O)$ curve (Fig. 3(b)) also looks quite reasonable. In particular, the slower fall of γ_R at higher oxygen fluxes reflects the “saturation” of R26 and R27 reaction rates due to the limited overall amount of adsorption sites on the etched surface.

CONCLUSIONS

The aim of this work was to investigate how the CF_4/C_4F_8 ratio in $CF_4 + C_4F_8 + O_2$ gas mixture influences electro-physical plasma parameters, steady-state densities of active species and silicon etching kinetics under typical reactive-ion etching conditions. Plasma modeling together with plasma diagnostics by Langmuir probes and optical emission spectroscopy confirms known features of F atom kinetics in both CF_4 and C_4F_8 plasmas in the presence of oxygen as well as provided the detailed analysis of plasma chemistry in the three-component gas mixture. In particular, it was found that the substitution of CF_4 by C_4F_8 at the constant fraction of O_2 causes the weak disturbance of electron temperature and plasma density (due to no principal changes in both electron energy loss channels and total ionization frequency), provides rapidly increasing density of fluorocarbon radicals as well as suppresses the F atom density. The last two phenomena are due to simultaneous changes in formation and loss rates for corresponding particles. Etching experiments demonstrate the monotonic decrease in Si etching rate toward C_4F_8 -rich plasmas. The analysis of heterogeneous process kinetics using model-predicted fluxes of plasma active species indicated a) the growth of polymer deposition rate and film thickness; b) the domination of chemical etching pathway for silicon (more than 85% from total etching rate); and c) an increase in the effective probability for $Si + xF \rightarrow SiF_x$ reaction. The last effect may be attributed to the weakening of surface passivation by oxygen atoms.

The work was supported by the Russian Science Foundation grant № 22-29-00216, <https://rscf.ru/project/22-29-00216/>.

The authors declare the absence a conflict of interest warranting disclosure in this article.

Исследование выполнено за счет гранта Российского научного фонда № 22-29-00216, <https://rscf.ru/project/22-29-00216/>.

Авторы заявляют об отсутствии конфликта интересов, требующего раскрытия в данной статье.

REFERENCES ЛИТЕРАТУРА

1. **Nojiri K.** Dry etching technology for semiconductors. Tokyo: Springer Internat. Publ. 2015. 116 p. DOI: 10.1007/978-3-319-10295-5.
2. **Wolf S., Tauber R.N.** Silicon Processing for the VLSI Era. V. 1. Process Technology. New York: Lattice Press. 2000. 416 p.
3. **Donnelly V.M., Kornblit A.** Plasma etching: Yesterday, today, and tomorrow. *J. Vac. Sci. Technol.* 2013. V. 31. P. 050825-48. DOI: 10.1116/1.4819316.
4. Advanced plasma processing technology. New York: John Wiley & Sons Inc. 2008. 479 p.
5. **Lieberman M.A., Lichtenberg A.J.** Principles of plasma discharges and materials processing. New York: John Wiley & Sons Inc. 2005. 757 p. DOI: 10.1002/0471724254.
6. **Kastenmeier B.E.E., Matsuo P.J., Oehrlein G.S.** Highly selective etching of silicon nitride over silicon and silicon dioxide. *J. Vac. Sci. Technol. A.* 1999. V. 17. P. 3179-3184. DOI: 10.1116/1.582097.
7. **Standaert T.E.F.M., Hedlund C., Joseph E.A., Oehrlein G.S., Dalton T.J.** Role of fluorocarbon film formation in the etching of silicon, silicon dioxide, silicon nitride, and amorphous hydrogenated silicon carbide. *J. Vac. Sci. Technol. A.* 2004. V. 22. P. 53-60. DOI: 10.1116/1.1626642.
8. **Schaepkens M., Standaert T.E.F.M., Rueger N.R., Sebel P.G.M., Oehrlein G.S., Cook J.M.** Study of the SiO_2 -to- Si_3N_4 etch selectivity mechanism in inductively coupled fluorocarbon plasmas and a comparison with the SiO_2 -to-Si mechanism. *J. Vac. Sci. Technol. A.* 1999. V. 17. P. 26-37. DOI: 10.1116/1.582108.
9. **Efremov A., Murin D., Kwon K.-H.** Concerning the Effect of Type of Fluorocarbon Gas on the Output Characteristics of the Reactive-Ion Etching Process. *Russ. Microelectronics.* 2020. V. 49. N 3. P. 157-165. DOI: 10.1134/S1063739720020031.
10. **Ефремов А.М., Мурин Д.Б., Кwon К.Х.** Параметры плазмы и кинетика активных частиц в смеси $CF_4+C_4F_8+Ar$. *Изв. вузов. Химия и хим. технология.* 2018. Т. 61. Вып. 4-5. С. 31–36. **Ефремов А.М., Мурин Д.Б., Кwon К.-Н.** Plasma parameters and active species kinetics in $CF_4+C_4F_8+Ar$ gas mixture. *ChemChemTech [Izv. Vyssh. Uchebn. Zaved. Khim. Khim. Tekhnol.]*. 2018. V. 61. N 4-5. P. 31-36. DOI: 10.6060/tcct.20186104-05.5695.
11. **Kimura T., Ohe K.** Model and probe measurements of inductively coupled CF_4 discharges. *J. Appl. Phys.* 2002. V. 92. P. 1780-1787. DOI: 10.1063/1.1491023.
12. **Rauf S., Ventzek P.L.** Model for an inductively coupled Ar/ C_4F_8 plasma discharge. *J. Vac. Sci. Technol. A.* 2002. V. 20. P. 14-23. DOI: 10.1116/1.1417538.

13. **Marra D.C., Aydil E.S.** Effect of H₂ addition on surface reactions during CF₄/H₂ plasma etching of silicon and silicon dioxide films. *J. Vac. Sci. Technol. A*. 1997. V. 15. P. 2508-2516. DOI: 10.1116/1.580762.
14. **Knizikevicius R.** Real dimensional simulation of SiO₂ etching in CF₄ + H₂ plasma. *Appl. Surface Sci.* 2004. V. 222. P. 275-285. DOI: 10.1016/S0042-207X(01)00413-4.
15. **Efremov A., Lee B.J., Kwon K.-H.** On Relationships Between Gas-Phase Chemistry and Reactive-Ion Etching Kinetics for Silicon-Based Thin Films (SiC, SiO₂ and Si_xN_y) in Multi-Component Fluorocarbon Gas Mixtures. *Materials*. 2021. V. 14. P. 1432(1-27). DOI: 10.3390/ma14061432.
16. **Kimura T., Noto M.** Experimental study and global model of inductively coupled CF₄/O₂ discharges. *J. Appl. Phys.* 2006. V. 100. P. 063303 (1-9). DOI: 10.1063/1.2345461.
17. **Chun I., Efremov A., Yeom G.Y., Kwon K.-H.** A comparative study of CF₄/O₂/Ar and C₄F₈/O₂/Ar plasmas for dry etching applications. *Thin Solid Films*. 2015. V. 579. P. 136-143. DOI: 10.1016/j.tsf.2015.02.060.
18. **Lim N., Efremov A., Kwon K.-H.** A comparison of CF₄, CHF₃ and C₄F₈ + Ar/O₂ Inductively Coupled Plasmas for Dry Etching Applications. *Plasma Chem. Plasma Process.* 2021. V. 41. P. 1671-1689. DOI: 10.1007/s11090-021-10198-z.
19. **Baek S.Y., Efremov A., Bobylev A., Choi G., Kwon K.-H.** On relationships between plasma chemistry and surface reaction kinetics providing the etching of silicon in CF₄, CHF₃, and C₄F₈ gases mixed with oxygen. *Materials*. 2023. V. 16. P. 5043(1-18). DOI: 10.3390/ma16145043.
20. **Shun'ko E.V.** Langmuir probe in theory and practice. Boca Raton: Universal Publ. 2008. 245 p.
21. **Lopaev D.V., Volynets A.V., Zyryanov S.M., Zotovich A.I., Rakhimov A.T.** Actinometry of O, N and F atoms. *J. Phys. D: Appl. Phys.* 2017. V. 50. P. 075202(1-17). DOI: 10.1088/1361-6463/50/7/075202.
22. **Engeln R., Klarenaar B., Guitella O.** Foundations of optical diagnostics in low-temperature plasmas. *Plasma Sources Sci. Technol.* 2020. V. 29. P. 063001 (1-14). DOI: 10.1088/1361-6595/ab6880.
23. **Cunge G., Ramos R., Vempaire D., Touzeau M., Neijbauer M., Sadeghi N.** Gas temperature measurement in CF₄, SF₆, O₂, Cl₂, and HBr inductively coupled plasmas. *J. Vac. Sci. Technol. A*. 2009. V. 27. N 3. P. 471-478. DOI: 10.1116/1.3106626.
24. **Vasenkov A.V., Li X., Oehlein G.S., Kushner M.J.** Properties of c-C₄F₈ inductively coupled plasmas. II. Plasma chemistry and reaction mechanism for modeling of Ar/c-C₄F₈/O₂ discharges. *J. Vac. Sci. Technol. A*. 2004. V. 22. P. 511-530. DOI: 10.1116/1.1697483.
25. **Hsu C.C., Nierode M.A., Coburn J.W., Graves D.B.** Comparison of model and experiment for Ar, Ar/O₂ and Ar/O₂/Cl₂ inductively coupled plasmas. *J. Phys. D: Appl. Phys.* 2006. V. 39. P. 3272-3284. DOI: 10.1088/0022-3727/39/15/009.
26. **Efremov A.M., Kim D.-P., Kim C.-I.** Simple model for ion-assisted etching using Cl₂/Ar inductively coupled plasma: effect of gas mixing ratio. *IEEE Trans. Plasma Sci.* 2004. V. 32. N 3. P. 1344-1351. DOI: 10.1109/TPS.2004.828413.
27. **Raju G.G.** Gaseous electronics. Tables, Atoms and Molecules. Boca Raton: CRC Press. 2012. 790 p. DOI: 10.1201/b11492.
28. **Christophorou L.G., Olthoff J.K.** Fundamental electron interactions with plasma processing gases. New York: Springer Science+Business Media LLC. 2004. 776 p. DOI: 10.1007/978-1-4419-8971-0.
29. **Ефремов А.М., Бетелин В.Б., Медников К.А., Кwon К.-Н.** Параметры плазмы и концентрации активных частиц в смесях фторуглеродных газов с аргоном и кислородом. *Изв. вузов. Химия и хим. технология*. 2021. Т. 64. Вып. 7. С. 46-53. DOI: 10.6060/ivkkt.20216407.6390.
30. **Ефремов А.М., Соболев А.М., Кwon К.-Н.** Особенности кинетики реактивно-ионного травления SiO₂ в смесях CF₄+ Ar + O₂ и C₄F₈+ Ar + O₂. *Изв. вузов. Химия и хим. технология*. 2020. Т. 63. Вып. 9. С. 21-27.
31. **Efremov A.M., Sobolev A.M., Kwon K.-H.** Features of SiO₂ reactive-ion etching kinetics in CF₄ + Ar + O₂ and C₄F₈ + Ar + O₂ gas mixtures. *ChemChemTech [Izv. Vyssh. Uchebn. Zaved. Khim. Khim. Tekhnol.]*. 2020. V. 63. N 9. P. 21-27. DOI: 10.6060/ivkkt.20206309.6198.
32. **Seah M.P., Nunney T.S.** Sputtering yields of compounds using argon ions. *J. Phys. D: App. Phys.* 2010. V. 43. N 25. P. 253001(1-24). DOI: 10.1088/0022-3727/43/25/253001.

Поступила в редакцию 02.10.2023

Принята к опубликованию 29.11.2023

Received 02.10.2023

Accepted 29.11.2023